Thermal diffusivity measurements of porous methane hydrate and hydrate-sediment mixtures

P. Kumar

Institute of Engineering and Ocean Technology (IEOT), Oil and Natural Gas Corporation (ONGC), Panvel, Navi Mumbai, India

D. Turner and E. D. Sloan

Center for Research on Hydrates and Other Solids, Colorado School of Mines, Golden, Colorado, USA

Received 28 August 2003; revised 22 September 2003; accepted 8 October 2003; published 28 January 2004.

[1] An experiment has been constructed to measure thermal diffusivity of methane hydrate and methane hydrate-sand/sediment mixtures. Thermal diffusivities of porous methane hydrate (40% pore space filled with methane gas) and mixtures of methane hydrate with Platte Valley sand and Blake Ridge sediment have been measured between the temperature range 265 K and 281 K, at pressures between 4.35 and 7.65 MPa. Thermal diffusivities of porous methane hydrate ranged between 3.1×10^{-7} and 3.3×10^{-7} m^2/s. Thermal diffusivity of 0.4 porosity methane hydrate was found to have inverse dependence on temperature, whereas the thermal diffusivity of methane hydrate-sediment/sand mixtures has positive temperature dependence. Thermal diffusivity of methane hydrate-sand/sediment mixtures increased with increasing hydrate volume fraction to a maximum between about 30 and 35 vol% in sand and between about 20 and 40 vol% in sediment. After the maxima, the thermal diffusivities decreased with increasing hydrate volume fraction. *INDEX TERMS:* 0930 Exploration Geophysics: Oceanic structures; 3022 Marine Geology and Geophysics: Marine sediments—processes and transport; 3939 Mineral Physics: Physical thermodynamics; 4215 Oceanography: General: Climate and interannual variability (3309); 5134 Physical Properties of Rocks: Thermal properties; *KEYWORDS:* methane hydrate, thermal diffusivity, sediment, methane, heat transport, conduction

Citation: Kumar, P., D. Turner, and E. D. Sloan (2004), Thermal diffusivity measurements of porous methane hydrate and hydrate-sediment mixtures, *J. Geophys. Res.*, *109*, B01207, doi:10.1029/2003JB002763.

1. Introduction

[2] Natural gas hydrate consists of hydrogen-bonded water cages containing small natural gas molecules. These clathrates have been found in sediments worldwide wherever low temperature, high pressure, water, and natural gas concentrations are conducive to their formation. Hydrate is known to exist in great quantities within the seafloor and permafrost regions of the world [*Collett and Kvenvolden*, 1987; *Kvenvolden et al.*, 1993]. It has been found to exist in massive, vein (layered), nodular, and dispersed form within a sediment matrix [*Malone*, 1985]. Hydrate-sediment mixture thermal properties have three major applications: (1) energy recovery, (2) climate change, and (3) seafloor stability.

[3] Although naturally occurring hydrate is considered as a possible source of future energy, it has also recently been found to be a global carbon cycle contributor, acting as a buffer against greenhouse gases [*Sassen et al.*, 2001; *Dickens*, 2002]. Seafloor hydrate is thought to be volatile [*Paull et al.*, 2000b]. It usually exists near its equilibrium conditions; therefore, relatively small disturbances, such as slight warming of water currents or pressure pulsing from tides, could sufficiently modify seafloor temperature or pressure to dissociate hydrate. Because gas hydrate stability is more susceptible to temperature changes than pressure, measurements constraining thermal regimes in hydrate bearing reservoirs provide fundamental information about parameters controlling stability of hydrate deposits.

[4] Gases released from hydrates expand approximately 180 fold under standard conditions [*Paull and Ussler*, 2001], so seafloor dissociation can potentially release large amounts of methane, a greenhouse gas, to the atmosphere [*Dickens*, 2001]. Also, disruption of the hydrate matrix can possibly cause seafloor slumping [*Kennett and Fackler-Adams*, 2000].

[5] Combining thermal property measurements with predictive models for the distribution and concentration of hydrate [*Xu and Ruppel*, 1999] constrains the migration of hydrate dissociation fronts in marine sediments. Thus the thermal property measurement of hydrate-bearing sediments provide necessary inputs for assessing sea floor stability, global climate change, sedimentation, erosion, submarine slide formation or other processes [*Ruppel*, 2000].

[6] Thermal properties of gas hydrate have not been extensively measured. Previous studies concentrated on the thermal conductivity of structure-II hydrate e.g., propane, THF [*Ross et al.*, 1981; *Ross and Andersson*, 1982].

0148-0227/04/2003JB002763$09.00

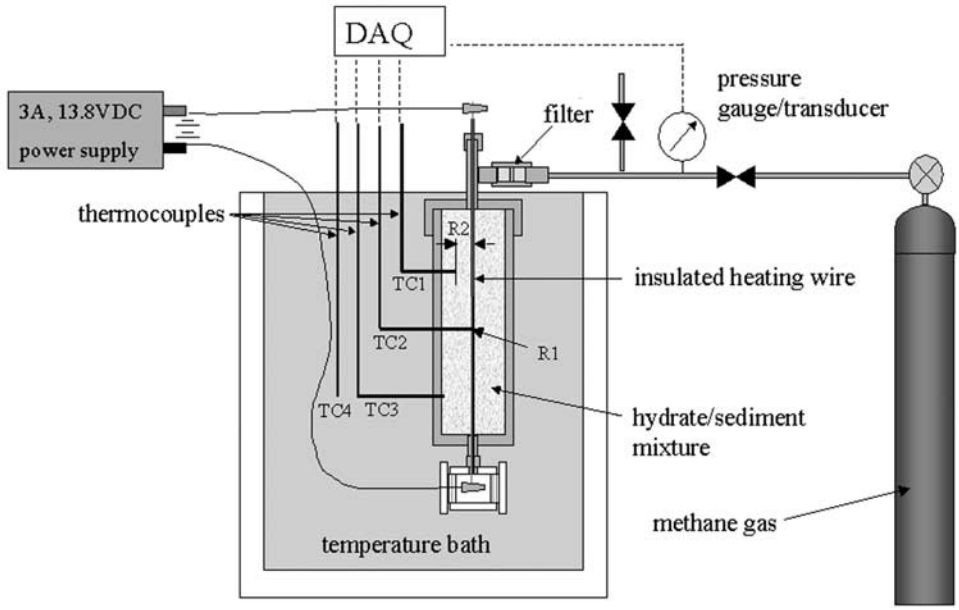

Figure 1. Experimental setup for thermal diffusivity measurements. The symbol "TC" represents thermocouples and R represents radial distance from the heating element. Modified from *Turner et al.* [2003].

While a few studies have been carried out on the measurement of thermal conductivity of structure I methane hydrate [*Cook and Leaist*, 1983], these investigations are at temperatures and pressures not representing natural gas hydrate settings. Recently, thermal conductivities of methane hydrate and sand mixtures have been measured [*deMartin*, 2001; *Waite et al.*, 2002]. Methane hydrate thermal diffusivity data are scarce; there is one published data set on thermal diffusivity of methane hydrate [*deMartin*, 2001], and no published thermal diffusivity data are available of methane hydrate-sand/sediment mixtures.

[7] An experiment has been assembled to measure the thermal diffusivity of hydrate and hydrate-sand/sediment mixtures. The thermal diffusivities of porous methane hydrate, methane hydrate-sand mixtures, and methane hydrate-sediment mixtures have been measured in the temperature range between 265 K and 282 K. The effects of temperature, sediment type and volume fraction on the heat transfer characteristics of methane hydrate have been studied and the data are presented herein.

2. Experimental Technique

[8] The thermal diffusivity experiment was based on the cylindrical Navier-Stokes heat equation, which relates temperature change with time at two locations in the hydrate-sediment mix to the thermal diffusivity. The details of the thermal diffusivity measurement technique and calibration are given by *Turner et al.* [2003]. However, the technique is summarized below.

[9] The following assumptions are applied to the general Navier-Stokes heat equation: (1) No volumetric heat generation occurs in the sample (however, line generation from the heating element); (2) no viscous dissipation; (3) axially long cell relative to radial dimension; (4) axial symmetry; (5) heat wave does not reach cell wall.

[10] With these assumptions, the Navier-Stokes equation reduces to the following:

$$\frac{\partial T}{\partial t} = \alpha\left[\frac{1}{r}\frac{\partial}{\partial r}\left(r\frac{\partial T}{\partial r}\right) + \frac{\partial^2 T}{\partial z^2}\right]. \quad (1)$$

[11] In equation (1) above, α is the thermal diffusivity, and T is temperature at time t, radial distance r, and axial location z. If temperature change with time is linear (especially true for short times), then by using the symmetry condition, equation (1) can be integrated to produce the following:

$$\alpha \cong \frac{\left[\frac{\Delta T}{\Delta t}R^2\right]_2 - \left[\frac{\Delta T}{\Delta t}R^2\right]_1}{4(T_2 - T_1)}. \quad (2)$$

T_1 and T_2 are average temperatures at two radial locations R_1 and R_2, respectively over time increment Δt. T_2, T_1, R_2 and R_1 and time are measurable, so thermal diffusivity can be calculated using equation (2).

3. Experimental Setup

[12] The experimental setup for measuring methane hydrate and hydrate-sand/sediment thermal diffusivities is shown schematically in Figure 1. The apparatus was a 20 cm inner length stainless steel cell with inner diameter 4.9 cm, wall thickness 0.3 cm and 350 ml internal volume. The cell was placed in the temperature-controlled propylene glycol/water bath. A Neslab® immersion cooler and 1000 W immersion heater controlled the bath temperature to +0.2 K fluctuations. An Omega® pressure transducer (PT) was used to continuously monitor cell pressure. Temperatures were measured by using four type-T thermocouples.

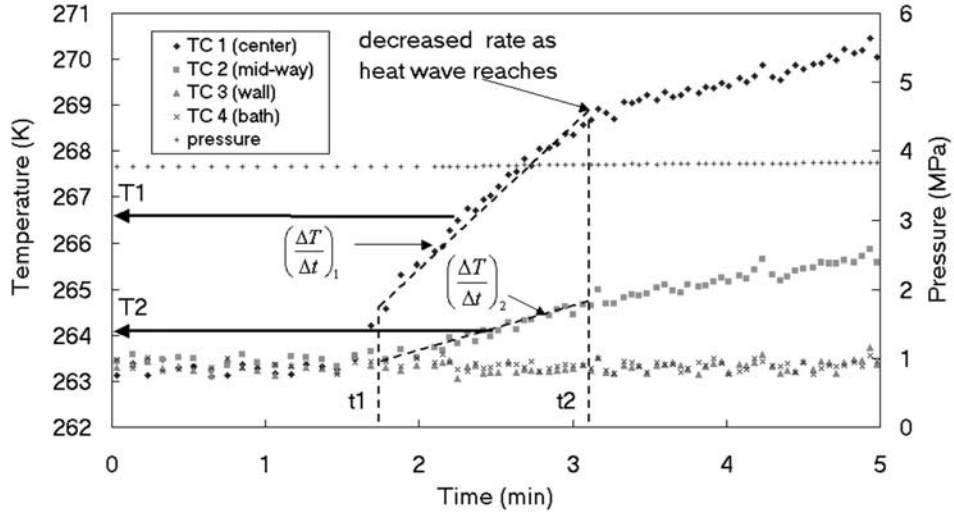

Figure 2. Example thermal diffusivity experiment of a hydrate-sediment mixture. The temperature response at two locations with time is related to the thermal diffusivity of the transporting medium.

[13] The heating element was an 18-gage (0.1016 cm diameter) Omega® resistance heating-wire. The wire was a 60% nickel and 16% chromium alloy with 1.384 Ohm/m resistance at 293 K. The wire was electrically insulated with a thin polypropylene heat-shrinkable coating. A 13.8VDC/3A power supply unit heated the wire during experiments. Ultra-pure methane gas (99.99% methane) was used in all experiments.

[14] Methane hydrate was formed directly within the cell from granular ice (sieved between 250 and 500-micron grain sizes) for the experiments using the *Stern et al.* [1996, 1998, 2000] method. (It should be noted that although this technique is commonly used for forming laboratory hydrate, hydrate formed in this manner might not represent hydrate formed from two phases in nature [*Huo et al.*, 2003].

[15] Blake Ridge site 996 B sediments (obtained during Ocean Drilling Program Leg 164) were used in the sediment and hydrate-sediment experiments. These samples consisted of 75% clay, 20% silt and 5% sand [*Paull et al.*, 2000a]. Commercially available quartz sand (density ~2.63 g/cc) from Platte Valley, Colorado, was used for sand and hydrate-sand experiments. Sand and sediment samples were sieved to between 250 and 500-micron grain sizes before use, so that mixture porosities could be easily determined. Sediment-ice sample porosity was calculated to be between 0.40 and 0.42 in all experiments.

[16] Sediment/sand samples were cooled with liquid nitrogen prior to mixing with ice particles to prevent melting. The ice and sediment/sand particles were mixed in a Hamilton Beach® mixer under liquid nitrogen to ensure uniform distribution of ice and sediment/sand particles. The cell, with thermocouple fittings, was also pre-cooled with liquid nitrogen. The cell was filled with sample material and placed immediately in the temperature bath (cooled to below 273 K).

[17] The cell was pressurized with methane and allowed to equilibrate at the bath temperature. Pressure was raised to between 4.35 and 7.65 MPa, respective of exceeding hydrate thermodynamic stability at the thermal diffusivity temperature desired. The bath temperature was increased slowly above the ice point to accelerate hydrate formation. Gas consumption rates showed very little hydrate formation at lower temperatures, but formation was highly accelerated near the ice point. The system was allowed to equilibrate at this temperature for several hours with occasional methane re-pressurization. Cycling the temperature across the ice point 2–3 times assisted in complete hydrate formation (by about ±2 K from 273 K). Hydrate formation was considered complete when no further gas was consumed and no temperature anomalies, typically associated with a phase change, were detected by the thermocouples in the sample.

[18] The degree of ice conversion to methane hydrate was calculated. The consumed methane mole fraction was determined using the Peng-Robinson equation of state [*Peng and Robinson*, 1976] and comparing to mass balance conversion (assuming all of the cages in the hydrate structure were filled with methane). In one experiment, the methane gas released upon hydrate dissociation was also measured, and the mole fraction values thus obtained were used for calculating degree of hydrate formation. These calculations showed that in our experiments, 100% ± 1% of ice was converted to hydrate.

4. Thermal Diffusivity Experiments

[19] Thermal diffusivities of methane hydrate, water saturated sediment, water-saturated sand, methane hydrate-sediment mixtures, and methane hydrate-sand mixtures were measured at various hydrate fractions and temperatures. Thermal diffusivity was measured in the temperature range between 265 K and 281 K and pressure between 4.35 and 7.65 MPa. A typical experimental cycle and temperature-pressure-time plot for these experiments is shown in Figure 2.

[20] A 3A current was passed through the resistor wire to generate heat in a methane hydrate or hydrate-sediment mixture as shown in Figure 1. This current was observed to be large enough to produce significant temperature

Table 1. Thermal Diffusivity of Porous Methane Hydrate[a]

Temperature, K	Pressure, Mpa	Thermal Diffusivity $\times 10^7$, m^2/s
265.3	4.34	3.3
269.4	4.38	3.2
274.2	4.38	3.2
281.7	6.79	3.1

[a]System is 60 vol% methane hydrate, 40 vol% methane gas.

change at the thermocouples before the heat wave reached the wall but low enough that the data acquisition system could retrieve sufficient data for analysis. The current used should have no bearing on the resulting thermal diffusivity, however.

[21] Thermocouples placed at the center (TC1), midway (TC2), and near the cell wall (TC3) sensed the temperature as the heat moved through the hydrate-sediment mixture in the cell. System temperatures and pressure were recorded with time as shown in Figure 2. The time for a typical thermal diffusivity experiment was about 180 seconds to 600 seconds, depending on the medium. Data used to calculate thermal diffusivity were that prior to the heat wave reaching the wall. There were two indications when the heat wave reached the wall: (1) The wall thermocouple (TC3) would register a temperature increase, and (2) the slope of temperature increase with time would change as the thermal diffusivity of the transporting medium changed to include the cooling fluid of the surrounding temperature bath (with convection).

[22] These two indicators cover the extreme boundary conditions. If convection at the wall were rapid, the kink would be predominant. In contrast, if convection at the wall were low, the temperature at the wall would increase. As can be seen in Figure 2, a kink in the temperature slope does occur. In many experiments, this kink was directly associated with a rise in wall temperature. Often, both phenomena occurred simultaneously, but slope change was a clearer indicator.

[23] In all experiments, sufficient system pressure was maintained (4.35–7.65 MPa) with methane gas well above the methane hydrate equilibrium pressure at the experimental temperatures. This was done to ensure that hydrate did not dissociate. The error in these experiments, measured by ice calibration, was found to be ±5% [*Turner et al.*, 2003].

[24] The temperature of a thermal diffusivity measurement was calculated as the average of the temperatures between the thermocouples, over the time of the experiment. More explicitly, the temperatures were averaged over the time of each experiment (assuming linearity of $\Delta T/\Delta t$), which are T_1 and T_2 in Figure 2. Then, the average of these temperatures was taken to be the measurement temperature.

[25] The thermal diffusivities of the following systems were measured: (1) 60 vol% methane hydrate, 40 vol% methane gas; (2) 60 vol% Blake Ridge site 996B sediment, 40 vol% water; (3) 48 vol% methane hydrate, 12 vol% sediment, 40 vol% methane gas; (4) 30 vol% methane hydrate, 30 vol% sediment, 40 vol% methane gas; (5) 60 vol% sediment, 40 vol% methane gas; (6) 60 vol% Platte Valley sand, 40 vol% water; (7) 42 vol% methane hydrate, 18 vol% sand, 40 vol% methane gas; (8) 30 vol% methane hydrate, 30 vol% sand, 40 vol% methane gas; and (9) 20 vol% methane hydrate, 40 vol% sand, 40 vol% methane gas.

Table 2. Thermal Diffusivity of Water-Saturated Platte Valley Sand and Sand-Methane Hydrate Mixtures

Temperature, K	Pressure, MPa	Thermal Diffusivity $\times 10^7$, m^2/s
40 vol% Water, 60 vol% Sand System		
266.5	0.21	2.1
273.6	0.21	2.2
282.4	0.21	2.6
18 vol% Sand, 42 vol% Methane Hydrate, 40 vol% Methane Gas System		
265.7	6.80	2.5
272.2	7.07	6.2
276.9	7.20	9.3
278.9	6.55	11.0
30 vol% Sand, 30 vol% Methane Hydrate, 40 vol% Methane Gas System		
268.9	5.39	5.4
272.2	5.46	7.6
272.8	5.46	8.0
273.4	5.38	8.4
276.0	5.46	9.9
40 vol% Sand, 20 vol% Methane Hydrate, 40 vol% Methane Gas System		
265.1	6.31	2.7
267.6	7.35	3.1
273.1	7.30	3.8
275.0	6.46	4.0
278.0	6.76	4.4

5. Results and Discussion

[26] Thermal diffusivity data of methane hydrate and methane hydrate-sand/sediment mixtures are presented in Tables 1 to 3. The results are discussed in the following sections.

5.1. Methane Hydrate System

[27] Thermal diffusivity of porous methane hydrate (40% pore filling methane gas) measured at five different temper-

Table 3. Thermal Diffusivity of Water-Saturated Blake Ridge Sediment and Sediment-Methane Hydrate Mixtures

Temperature, K	Pressure, MPa	Thermal Diffusivity $\times 10^7$, m^2/s
40 vol% Water, 60 vol% Sediment System		
261.9	0.21	2.0
274.6	0.21	2.1
293.5	0.21	2.6
12 vol% Sediment, 48 vol% Methane Hydrate, 40 vol% Methane Gas System		
268.9	5.59	3.5
274.1	5.66	3.6
278.1	5.89	3.8
30 vol% Sediment, 30 vol% Methane Hydrate, 40 vol% Methane Gas		
269.5	5.79	4.3
273.8	5.79	4.6
278.3	5.99	4.8
60 vol% Sediment, 40 vol% Methane Gas System		
300.1	0.21	0.97

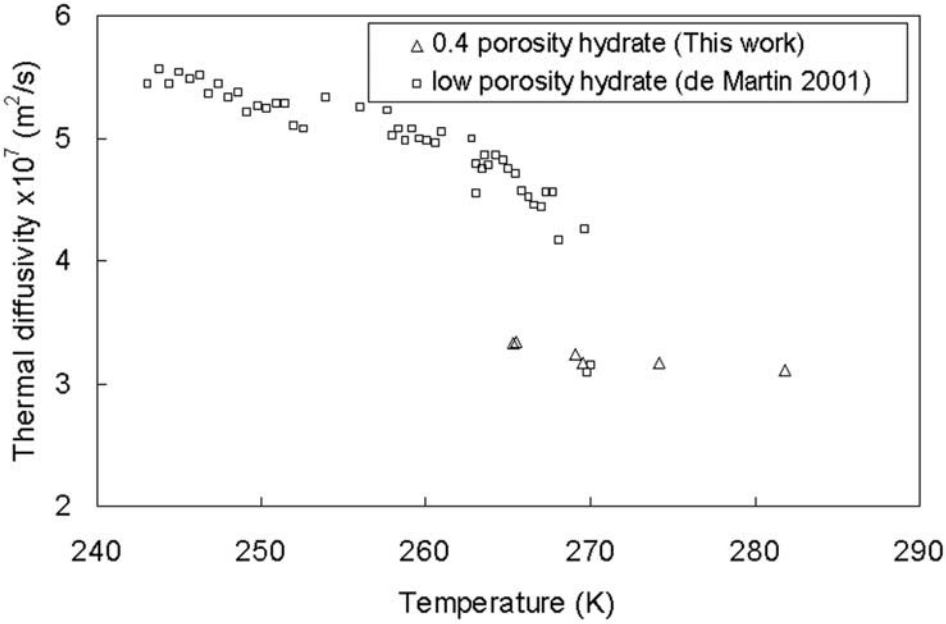

Figure 3. Thermal diffusivity of methane hydrate with temperature.

atures is shown in Figure 3. Porous methane hydrate thermal diffusivity had slightly negative temperature dependence. The negative dependence might have been caused by the presence of methane gas in the residual pores of the medium. Thermal diffusivity of methane-filled porous methane hydrate in this work was between 3.1×10^{-7} and 3.3×10^{-7} m^2/s.

[28] Thermal diffusivity data in this work were correlated with available literature data. Only one thermal diffusivity data set was available for methane hydrate [*deMartin*, 2001]. The thermal diffusivity data of methane hydrate from deMartin were higher than ours at lower temperatures but abruptly come closer at about 270 K. He has attributed this anomaly to ice contamination in the compacted hydrate sample [*deMartin*, 2001]. In addition, the hydrate in deMartin's work was formed differently from ours and was likely much less porous than our samples.

5.2. Methane Hydrate Sand/Sediment System

[29] Thermal diffusivities of water-saturated sediment, methane hydrate-sediment mixtures, water-saturated sand, and methane hydrate-sand mixtures were measured for various temperatures and hydrate volume fractions and are shown in Figure 4.

5.2.1. Effect of Temperature

[30] As discussed in section 5.1, thermal diffusivity of porous methane hydrate decreases with increasing temperature. However, it can be seen from Figure 4 that thermal

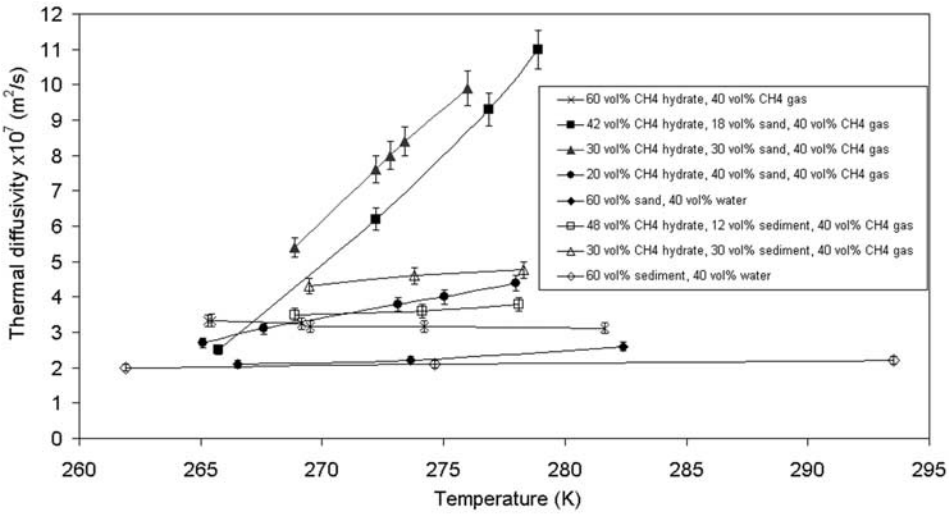

Figure 4. Thermal diffusivity of methane hydrate, water-saturated sand/sediment and methane hydrate-sand/sediment mixtures with temperature.

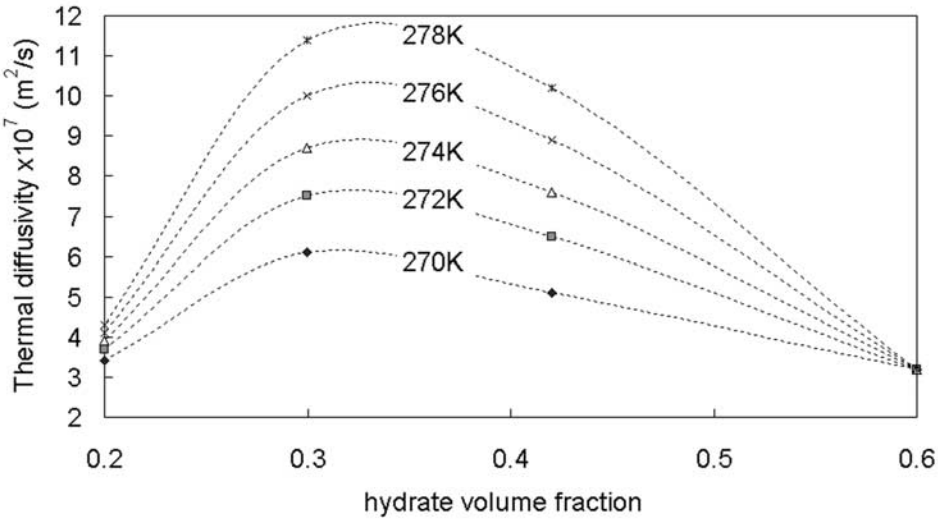

Figure 5. Thermal diffusivity with volume fraction of hydrate in the Platte Valley sand and 40 vol% pore-filling methane gas.

diffusivity of water-saturated sediment and sand increases with temperature. A similar trend was observed for 48 vol% methane hydrate-12 vol% sediment mixture and 30 vol% hydrate-30 vol% sediment mixture. Methane hydrate-sand systems (42 vol% hydrate-18 vol% sand mixture, 30 vol% hydrate-30 vol% sand mixture and 20 vol% hydrate-40 vol% sand mixture) also show positive dependence on temperature but the magnitude of temperature response was more than the hydrate-sediment mixture systems.

5.2.2. Effect of Sediment Type

[31] As shown in Figure 4, hydrate-sand thermal diffusivities are generally higher than hydrate-sediment thermal diffusivities. The higher temperature response of hydrate-sand from hydrate-sediment thermal diffusivity may have been because a larger sand particle resembles many smaller sediment particles that are fused together. For the same quantity of sand or sediment, the thermal transport is lower for the sediment with lower thermal contact. This may be significant while formulating thermal recovery schemes for hydrate production from sandy and/or clayey sediments.

5.2.3. Effect of Sediment/Sand Fraction

[32] Hydrate fraction effects on thermal diffusivity of methane hydrate-sand/sediment mixtures are shown in Figures 5 and 6, respectively. All data in Figure 5 are cross-plots of porous methane hydrate and methane hydrate-sand mixture systems where pore spaces are filled with methane gas.

[33] The points in Figure 6 are also cross-plots of porous methane hydrate and methane hydrate-sediment mixtures, except at 0 vol% hydrate, which are actual data. The pore spaces are also filled with methane gas in these systems.

[34] Figure 5 shows methane hydrate-sand mixture thermal diffusivities for various hydrate volume fractions and

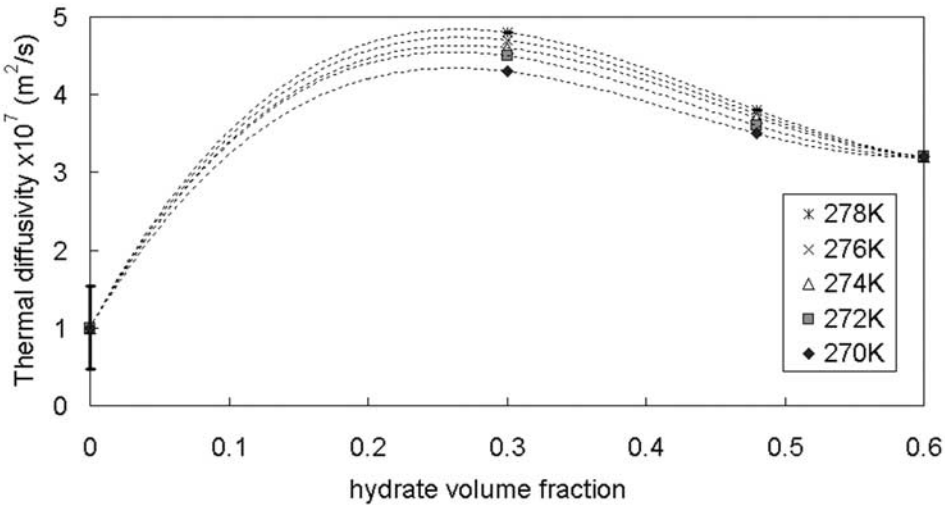

Figure 6. Thermal diffusivity with hydrate volume fraction of hydrate in the Blake Ridge sediment and 40 vol% pore-filling methane gas.

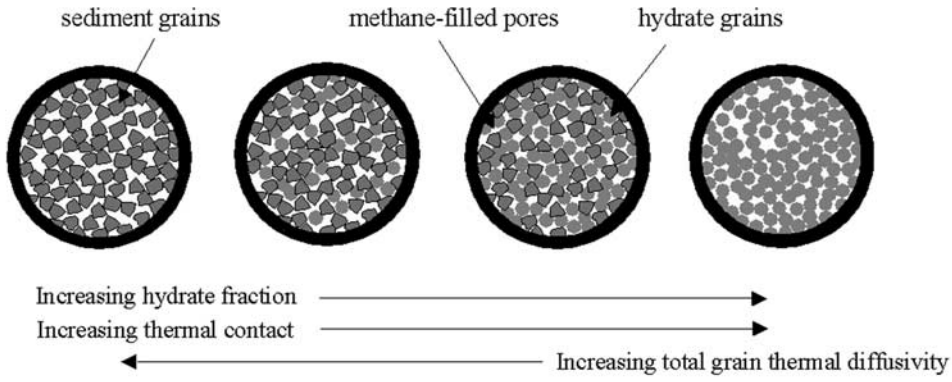

Figure 7. Illustration showing the effect of hydrate fraction in sediment in the porous system. Sediment grains have high thermal diffusivity, but poor thermal contact. Hydrate grains create good thermal contacts, but have lower thermal diffusivity than the sediments grains.

temperatures. Figure 6 shows methane hydrate-sediment thermal diffusivities for various hydrate volume fractions and temperatures. Thermal diffusivity first increases with increasing hydrate fraction but decreases after a certain volume fraction of hydrate in sand/sediment. The maximum thermal diffusivity is at a methane hydrate fraction between 30 and 35 vol% in sand with 40 vol% pore gas and between 20 and 40 vol% in sediment with 40 vol% pore gas. Similar trends exist at temperatures from 270 K to 278 K.

[35] One hypothesis explains the maximum thermal diffusivity in methane hydrate with sand/sediment fraction, which is illustrated in Figure 7. Thermal diffusivity of sand/sediment grains was higher than that of hydrate grains. Thermal diffusivity of the mixtures increased with hydrate fraction because hydrate fused together the sand/sediment grains, thereby enhancing inter-granular contact. However, when the methane hydrate amount was more than 30 vol% (with 40 vol% pore gas), the amount of lower-thermal diffusivity hydrate dominated over the higher-thermal diffusivity sediment, resulting in lower thermal diffusivity with hydrate fraction.

6. Conclusions

[36] The following conclusions summarize the thermal diffusivity experiments on porous methane hydrate, methane hydrate-sand mixtures, and methane hydrate-sediment mixtures:

[37] 1. Thermal diffusivity of porous methane hydrate (~60 vol%) and methane pore gas (~40 vol%) had an inverse dependence on temperature, whereas the thermal diffusivity of water-saturated sand/sediment (~60 vol% solids, ~40 vol% water) had positive temperature dependence.

[38] 2. Methane hydrate-sand/sediment thermal diffusivity increased with hydrate fraction to a maximum between 30 and 35 vol% in sand and pore gas and between 20 and 40 vol% in sediment and pore gas; thereafter, it decreased with increasing hydrate volume fraction.

[39] 3. Sediment type influenced the heat transport properties of methane hydrate mixtures. Thermal diffusivity of a methane hydrate-sediment mixture increased when the sediment type changed from sediment to sand at the same hydrate fraction. The hydrate distributed in sandy sediment will dissociate faster than those in clayey sediments.

[40] Hydrate volume fraction in sediment is significant for seafloor thermal modeling, such as seafloor stability or gas release modeling, since it dictates transport times. The fastest rate for thermal transport occurs at the maximum thermal diffusivity. Therefore the Blake Ridge should be least stable at between 20 and 40 vol% hydrate. A location with coarser sediments typical of the Platte Valley sand would be least stable at between 30 and 35 vol% hydrate fraction.

[41] In locations where warm-water current or tidal effects shift local hydrated seafloor equilibrium conditions, fine grain sediments are more stable than coarse grain sediments.

[42] **Acknowledgments.** The authors are thankful to the Oil and Natural Gas Corporation Limited and National Gas Hydrate Program of India, British Petroleum, ChevronTexaco, ConocoPhillips, Halliburton, and Unocal for sponsoring this work at Colorado School of Mines, USA. The authors are also thankful to T. S. Collett of United States Geological Survey for providing sediment samples from ODP Leg 164 Site 996B.

References

Collett, T. S., and K. A. Kvenvolden (1987), Evidence of naturally occurring gas hydrate on the North Slope of Alaska, *U. S. G. S. Open File Rep. 87-255*, *8*.

Cook, J. G., and D. G. Leaist (1983), An exploratory study of the thermal conductivity of methane hydrates, *Geophys. Res. Lett.*, *10*, 397–399.

deMartin, B. J. (2001), Laboratory measurement of the thermal conductivity and thermal diffusivity of methane hydrate at simulated in-situ conditions, Master thesis, Georgia Inst. of Technol., Atlanta, Ga.

Dickens, G. R. (2001), The potential volume of oceanic methane hydrates with variable external conditions, *Org. Geochem.*, *32*, 1179–1193.

Dickens, G. R. (2002), The phanerozoic carbon cycle with a gas hydrate capacitor, *Geochim. Cosmochim. Acta*, *66*, A183.

Huo, Z., K. Hester, K. Miller, and D. Sloan (2003), Methane hydrate nonstoichiometry and phase diagram, *AIChE J.*, *49*, 1300–1306.

Kennett, J. P., and B. N. Fackler-Adams (2000), Relationship of clathrate instability to sediment deformation in the upper Neogene of California, *Geology*, *28*, 215–218.

Kvenvolden, K. A., G. D. Ginsburg, and V. A. Solovieiv (1993), Worldwide distribution of subaquatic gas hydrates, *Geomar. Lett.*, *13*, 32.

Malone, R. D. (1985), Gas hydrates topical report, *DOE/METC/SP-218*, U. S. Dept. of Energy, Morgantown, W. Va.

Paull, C. K., and W. Ussler III (2001), History and significance of gas sampling during DSDP and ODP drilling associated with gas hydrates, in *Natural Gas Hydrates: Occurrence, Distribution, and Detection*, *Geophys. Monogr.*, vol. 124, edited by C. K. Paull and W. P. Dillon, pp. 53–65, AGU, Washington, D. C.

Paull, C. K., , R. Matsumoto, P. J. Wallace, and W. P. Dillon (Eds.) (2000a), *Proceedings Ocean Drilling Program Scientific Results*, vol. 164, 615 pp., Ocean Drill. Program, College Station, Tex.

Paull, C. K., W. Ussler III, and W. P. Dillon (2000b), Potential role of gas hydrate decomposition in generating submarine slope failures, in *Natural Gas Hydrate in Oceanic and Permafrost Environments*, edited by M. D. Max, pp. 149–156, Kluwer Acad., Norwell, Mass.

Peng, D., and D. B. Robinson (1976), Two and three phase equilibrium calculations for systems containing water, *Can. J. Chem. Eng.*, *54*, 595–599.

Ross, R. G., and P. Andersson (1982), Clathrate and other solid phases in the tetrahydrofuran-water system: Thermal conductivity and heat capacity under pressure, *Can. J. Chem. Eng.*, *60*, 881–892.

Ross, R. G., P. Andersson, and G. Backstrom (1981), Unusual PT dependence of thermal conductivity for a clathrate hydrate, *Nature*, *290*, 322–323.

Ruppel, C. (2000), Thermal state of the gas hydrate reservoir, in *Natural Gas Hydrate in Oceanic and Permafrost Environments*, edited by M. D. Max, p. 29, Kluwer Acad., Norwell, Mass.

Sassen, R., S. T. Sweet, A. V. Milkov, D. A. DeFreitas, and M. C. Kennicutt II (2001), Stability of thermogenic gas hydrate in the Gulf of Mexico: Constraints on models of climate change, in *Natural Gas Hydrates: Occurrence, Distribution, and Detection*, *Geophys. Monogr.*, vol. 124, edited by C. K. Paull and W. P. Dillon, pp. 131–143, AGU, Washington, D. C.

Stern, L. A., S. H. Kirby, and W. B. Durham (1996), Peculiarities of methane clathrate hydrate formation and solid-state deformation, including possible superheating of water ice, *Science*, *273*, 1843–1848.

Stern, L. A., S. H. Kirby, and W. B. Durham (1998), Polycrystalline methane hydrate: Synthesis from superheated ice, and low temperature mechanical properties, energy and fuels, *Energy Fuels*, *12*, 201–211.

Stern, L. A., S. H. Kirby, W. B. Durham, S. Circone, and W. F. Waite (2000), Laboratory synthesis of pure methane hydrate suitable for measurement of physical properties and decomposition behavior, in *Natural Gas Hydrate in Oceanic and Permafrost Environments*, edited by M. D. Max, pp. 323–348, Kluwer Acad., Norwell, Mass.

Turner, D., P. Kumar, and E. D. Sloan (2003), A new technique for thermal diffusivity measurements in hydrate-sediment mixtures, paper presented at the Fifteenth Symposium on Thermophysical Properties, Natl. Inst. for Stand. and Technol., Boulder, Colo., USA, 22 –27 June.

Waite, W. F., J. Pinkston, and S. H. Kirby (2002), Preliminary laboratory thermal conductivity measurements in pure methane hydrate and hydrate-sediment mixtures: A progress report, paper presented at the Fourth International Conference on Gas Hydrates, Heat Transfer Soc. of Jpn., Yokohama, Japan, 19–23 May.

Xu, W., and C. Ruppel (1999), Predicting the occurrence, distribution and evolution of methane gas hydrate in porous marine sediments, *J. Geophys. Res.*, *104*, 5081–5096.

P. Kumar, Institute of Engineering and Ocean Technology (IEOT), Oil and Natural Gas Corporation (ONGC), Panvel, Navi Mumbai 410221, India. (pushpendra@ongc.net)

E. D. Sloan and D. Turner, Center for Research on Hydrates and Other Solids, Colorado School of Mines, 1600 Illinois Street, Golden, CO 80401, USA. (esloan@mines.edu; djturner@mines.edu)